GEOPHYSICAL RESEARCH LETTERS, VOL. 34, L13203, doi:10.1029/2007GL029754, 2007

High resolution mapping of TiO_2 abundances on the Moon using the Hubble Space Telescope

M. S. Robinson,[1] B. W. Hapke,[2] J. B. Garvin,[3] D. Skillman,[3] J. F. Bell III,[4] M. P. Ulmer,[5] and C. M. Pieters[6]

Received 20 February 2007; revised 10 May 2007; accepted 23 May 2007; published 7 July 2007.

[1] Samples of the lunar regolith returned by Apollo astronauts show large variations (0 to >10 wt%) in TiO_2 abundance indicating complex compositional zonation within the lunar mantle. A long held goal of the lunar science community is the accurate determination of TiO_2 abundances on the lunar surface through remote sensing methods. To date only limited progress has been made in this area using spacecraft spectral measurements acquired in visible through near-infrared wavelengths. Here we show that variations in the ratios of ultraviolet (UV) to visible (VIS) reflectances in images taken by the Hubble Space Telescope indicate a strong correlation with TiO_2 abundances determined from returned samples at the Apollo 17 landing site, and little correlation with the ''maturity'' of lunar soils. These new findings imply that UV-VIS observations may lead to an alternate and improved method of remotely mapping TiO_2-bearing materials (probably as ilmenite) across the lunar surface and enable more refined studies of lunar crustal composition, surface volcanism, and subsurface magma evolution processes. Additionally, accurate identification and quantification of TiO_2 rich deposits serves to guide future human exploration of the Moon. **Citation:** Robinson, M. S., B. W. Hapke, J. B. Garvin, D. Skillman, J. F. Bell III, M. P. Ulmer, and C. M. Pieters (2007), High resolution mapping of TiO_2 abundances on the Moon using the Hubble Space Telescope, *Geophys. Res. Lett.*, *34*, L13203, doi:10.1029/2007GL029754.

1. Introduction

[2] Early ground based telescopic UV-VIS measurements of the Moon indicated that major color units within the lunar mare could be mapped using remote sensing techniques [*Pieters*, 1978]. The link between color variation and compositional variation was established by studies that noted correlations between color (VIS/UV ratio) and the TiO_2 contents of the returned Apollo lunar samples [*Whitaker*, 1972; *Charette et al.*, 1974]. *Wells and Hapke* [1977] suggested that these correlations and associated spectral differences might in part be due to varying abundances of ilmenite ($FeTiO_3$) in lunar soils.

[3] Visible and near-infrared reflectance (400–2800 nm) of the lunar regolith is dominantly controlled by variations in the abundance of four components: (1) high albedo, low-iron minerals (largely anorthosite); (2) iron bearing silicate minerals (primarily pyroxene and olivine); (3) maturation products (complex glasses, coatings bearing nanophase metallic iron [*Hapke et al.*, 1975; *Pieters et al.*, 2000; *Hapke*, 2001]); and (4) opaque minerals (primarily ilmenite and spinel). Despite the spectral properties of ilmenite in visible and near-infrared reflectance, an accurate method for recovering estimates of TiO_2 abundance has eluded the lunar remote sensing community for over thirty years [*Gillis-Davis et al.*, 2006].

[4] The same components control the reflectance of the lunar regolith into the near-UV (250 to 400 nm) as well. Laboratory spectra show that Fe-bearing silicates and oxides have strong absorption bands in the UV [*Wells and Hapke*, 1977] and that ilmenite often exhibits a reflectivity upturn below about 450 nm [*Wagner et al.*, 1987] continuing well into the UV. Therefore, UV observations have the potential to constrain TiO_2 abundances in lunar soils.

[5] The Earth's atmosphere is essentially opaque below about 340 nm so ground-based telescopic observations of the UV reflectance of the Moon are problematic. Furthermore, no spacecraft to date has acquired lunar spectral observations with high spatial resolution in the UV, and thus the full potential of lunar compositional mapping in the UV has not been realized. The Hubble Space Telescope (HST), high above the Earth's atmosphere, provides a way to assess this potential with high spatial resolution, UV-sensitive instrumentation. We used the HST Advanced Camera for Surveys High Resolution Camera (ACS/HRC [*Pavlovsky et al.*, 2002]) to acquire UV-VIS images of three lunar targets to investigate relations between UV color variations and compositional units within lunar soils.

2. HST Observations

[6] The new HST lunar observations had two primary objectives: (1) assess the magnitude and spatial relations of contrast variations in the UV; and (2) assess the ability of UV reflectance to measure TiO_2 content within mare soils. Our HST multi-spectral lunar data consist of ACS/HRC four-filter observations (F250W, F344N, F502N, F658N) with an angular resolution of ~60 m/pixel of three targets: the Apollo 17 landing site, the Apollo 15 landing site, and the *Aristarchus* crater and plateau. The Apollo sites allow calibration of the HST measurements in association with known compositions of lunar soil samples.

[1]School of Earth and Space Exploration, Arizona State University, Tempe, Arizona, USA.
[2]Department of Geology and Planetary Science, University of Pittsburgh, Pittsburgh, Pennsylvania, USA.
[3]NASA Goddard Space Flight Center, Greenbelt, Maryland, USA.
[4]Department of Astronomy, Cornell University, Ithaca, New York, USA.
[5]Department of Physics and Astronomy, Northwestern University, Evanston, Illinois, USA.
[6]Department of Geological Sciences, Brown University, Providence, Rhode Island, USA.

0094-8276/07/2007GL029754$05.00

Table 1. Summary of HST ACS/HRC Lunar Observations

Target	Date, UT	Solar Latitude	Solar Longitude	Phase	Integration Time,[a] seconds
Apollo 17	2005-08-17	1.2°	34.8°	39°	4, 4, 1.5, 0.7
Apollo 15	2005-08-20	1.2°	357.3°	5°	4, 4, 1.5, 0.7
Aristarchus	2005-08-21	1.2°	346°	18°	4, 4, 1.5, 0.7

[a]Integration times in seconds for F250W, F344N, F502N, and F658N filters, respectively.

[7] Due to the rapid velocity of the HST relative to the Moon, and the limitation of HST to track at only one constant linear velocity, accurate pointing (and sharp images) can only be obtained during three brief periods per orbit when the apparent velocity of the lunar target is relatively constant. These periods occur when the HST, from the point of view of an observer at the lunar target, reaches maximum elongation (twice per orbit), and when HST makes its closest approach to the Earth-target line (once per orbit). Even during these periods, pointing uncertainties were equivalent to about one-half of an ACS frame (~35 km), thus each target was imaged as a 2 × 2 pattern with a fifth observation centered (for each filter) on the target to insure coverage. Operational timing constraints dictated that each filter set (5 images per target) had to be acquired at different times within an orbit and from adjacent orbits, resulting in at most 3.2° change of phase angle from the first image to the last image (across all 4 filter sets). Variation in phase angle within a filter set (5 images) was less than 0.8°. In addition, the orbital motion of HST can cause as much as 2.2° of variation in the angle between a target's local zenith and the line of sight to HST across all exposures.

[8] Despite these pointing and stability challenges, the HST observations were accomplished successfully (Table 1). For the Apollo 17 site, regions traversed and sampled by the astronauts were covered in all four wavelengths, as were significant portions of the surrounding regions. Due to the long exposures (4 seconds) required to obtain useful signal-to-noise for the two UV filters (F250W, F344N) and variable pointing stability, some of the UV images suffered significant motion smear (roughly 3 to 10 pixels). The angular resolution of a pixel projected on the surface of the Moon was ~60 m but the effective resolution varied depending on the wavelength-dependent point spread function and motion-induced smear. The effective wavelength (after accounting for detector quantum efficiency and the solar spectrum) for each filter is the same as the nominal wavelength (indicated as 3 digit number in filter name), except for the F250W filter which has an effective wavelength of ~290 nm for the lunar observations. This shift is due to the steeply falling solar spectrum at shorter wavelengths.

[9] Standard HST radiometric processing [*Pavlovsky et al.*, 2002] was applied to the lunar observations, yielding radiances for each pixel. To facilitate comparisons between these measurements and laboratory reflectance spectra of rocks and minerals, these radiances were then converted to radiance factor (I/F) [*Bell et al.*, 1997]. Instrumental geometric distortions were removed, and then the filter sets were co-registered using an automated subpixel scheme that employs a weighted least squares fit to account for local distortions. This strategy was dictated by significant parallax-induced distortions between filter sets. The final co-registered filter set was then projected to map coordinates through correlation with a Clementine (CL) multispectral mosaic (100 m/pixel). Gross parallax differences between the nadir looking CL observations (0° emission angle) and oblique HST observations (~20° emission angle) result in poor pixel-to-pixel matches between the two datasets, especially in regions of steep relief such as North and South Massifs at the Apollo 17 site. Thus, comparisons between the two datasets require manual selection of corresponding pixel boxes (rather than a strict co-registration of the two datasets).

3. Discussion

[10] A major question addressed was whether remote measurements in the UV can detect compositional variations in lunar soils (Figure 1). Figures 2a and 2b show the Apollo 17 area as imaged by CL (750 nm) and HST (502 nm). Figures 2c and 2d compare values of spectral ratios versus visible reflectance within each image. With the HST data, highland and mare materials are easily separated in terms of reflectance and UV contrast, and appear as distinct intersecting trends. The HST pattern grossly mimics trends seen in the CL data. However, differences between the two datasets indicate that the UV data reflects complementary or unique information. Note that a portion of greater scatter seen in the CL data may be an artifact due to small differences in *effective* resolution between the datasets and higher instrumental scattered light in the CL data [*Robinson et al.*, 2003].

[11] Regolith TiO_2 values from individual Apollo 17 soil sample stations were used to derive an absolute calibration for the HST UV ratio. Each individual sample station was

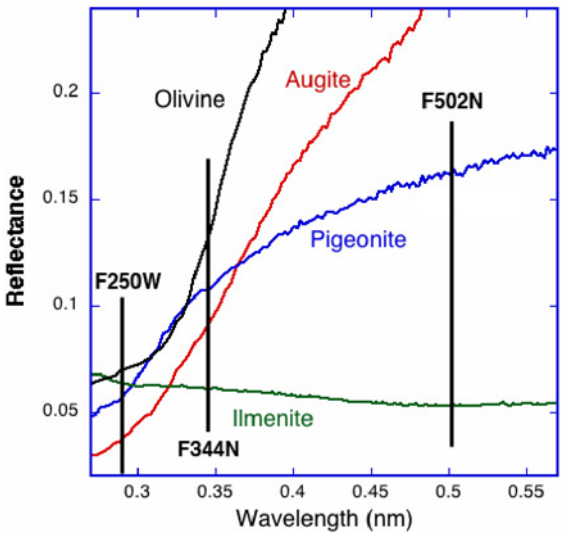

Figure 1. Spectra of mineral powders (from USGS spectral library) illustrating ilmenite's distinctive negative slope in the UV and VIS relative to typical iron-bearing silicates. Effective band centers of HST ACS/HRC filters shown as vertical lines.

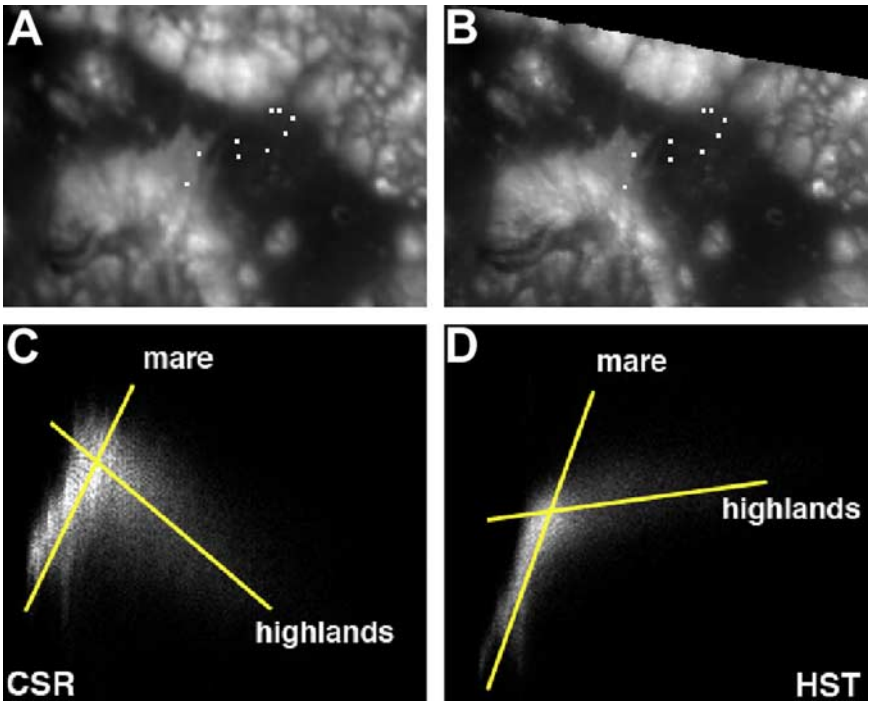

Figure 2. (a) CL 750 nm image of Apollo 17 area, boxes indicate stations shown in Figure 3, width 28 km. (b) HST 502 nm image of Apollo 17 area, boxes same as in Figure 2a. (c) CL scatter plot of data properties, x-axis 750 nm reflectance (0.03 to 0.11) y axis 750/415 nm ratio (1.4 to 1.8). (d) HST scatter plot, x-axis 502 nm reflectance (0.02 to 0.10) y-axis 502/250 nm ratio (1.7 to 2.3). Lines illustrate spectral trends for different terrains.

located manually in both the HST and CL images by comparison with published traverse maps and Apollo Pan photography. The reflectances were sampled by averaging over 3x3 pixel boxes at 100 m/pixel around the exact station locations. We estimate that the sample boxes contain the actual surface sample station location in all cases except possibly for the L5/L6 box. These two Lunar Roving Vehicle stations are found on relatively featureless light-toned mantle material. However by triangulating from nearby features we are confident that at least one of the stations is in the box and the other is within one pixel of the box. Regolith TiO_2 values from individual soil sample stations are plotted against the HST UV ratios (Figure 3) and a strong correlation is found (R = 0.979). Figure 3 also shows a similar plot for the CL 715/450 ratios—note the greater scatter from the correlation line for the CL-derived data relative to the HST data.

[12] The high correlation between the HST UV/VIS ratios and TiO_2 soil values implies that soil color is strongly controlled by variations in this parameter. The best-fit line in Figure 3 provided a calibration from the values in the HST ratio image to absolute TiO_2 wt.% and was used to generate the TiO_2 abundance map shown in Figure 4. The mare soils generally have TiO_2 values between 6 and 8 wt.%, while highland soils exhibit −1 to 2 wt.%. The mafic pyroclastic material proposed to be admixed in valley floors between some highland massifs [*Lucchitta*, 1972] shows 2-4 wt.% TiO_2. Several of the soils used in our analysis are dominantly feldspathic and relatively mature (S6, S7, L11) and are highly correlated with TiO_2 abundance. Significantly, even the two relatively immature feldspathic sample stations (S2A, L5/L6) also show a strong correlation, consistent with the hypothesis that the HST UV/

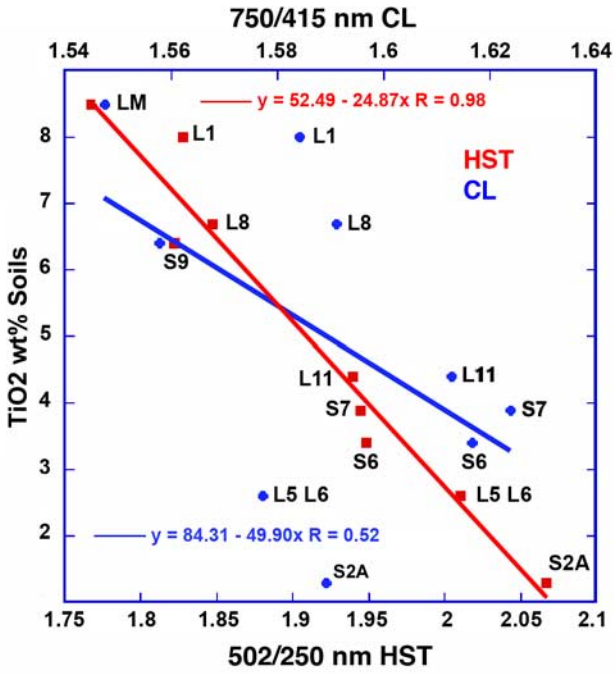

Figure 3. Spectral parameter plot for HST and CL for the Apollo 17 landing area. Location of sample areas indicated in true size (300 m × 300 m boxes) in Figure 2. S and L indicate formal sample stations and lunar rover stations, respectively. The red squares are the HST data; the blue dots are the CL data. The lines of corresponding color are the least squares regression straight line fitted to each data set. References for TiO_2 values summarized by *Robinson and Jolliff* [2002].

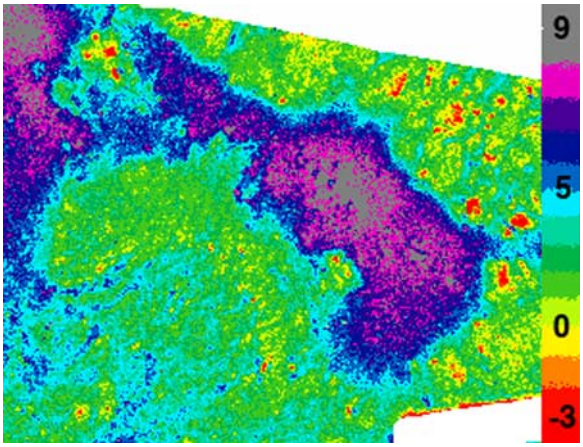

Figure 4. TiO_2 wt.% abundance map of Apollo 17 region (width 28 km) derived from HST UV ratio tied to Apollo soil sample analyses.

VIS ratio reflects TiO_2 abundance independent of soil maturity. Note that these same stations are not well correlated in the CL data (Figure 2), indicating significant wavelength-dependent maturity effects on the CL ratio.

[13] Most highland areas in the HST data exhibit derived TiO_2 values between 0 and 1 wt.%. The apparent negative TiO_2 values exhibited by some small highland patches indicate that the HST UV ratio correlation in Figure 3 is not valid for all highland units (UV ratios >2.1). Possible reasons include effects of maturity, non-linearity of compositional mixing, TiO_2 in augite and glasses (rather than ilmenite), or other effects due to unknown compositional differences. These apparent negative patches correlate with materials shown to have a low maturity calculated from CL methods described by *Lucey et al.* [2000]. The most negative values are associated with immature materials within distinctive highland material known as the Sculptured Hills, north and east of the landing site [*Robinson and Jolliff*, 2002]. With the existing remote sensing data and lack of returned samples for these units, it is not possible to definitively determine the cause of the negative values at this time.

[14] In contrast with most silicates, ilmenite has a relatively low albedo and flat spectrum in the UV and visible. Increasing ilmenite would thus decrease the albedo and the 502/250 ratio, as observed. The correlation of the color ratio with TiO_2 suggests that some form of ilmenite in the Apollo 17 mare and mixed mare-feldspathic soils is affecting the observed color. The HST UV/VIS ratio correlation with TiO_2 is less sensitive to maturity effects than the CL ratio, indicating improvements in accuracy over existing methods may be possible either directly through the simple ratio or a parameter derived from UV color. More extensive observations and detailed analyses are needed to determine if the HST UV/VIS ratio correlation with TiO_2 found in the Apollo 17 region is truly robust across large extents of lunar terrain. However, preliminary analysis of the Apollo 15 HST images is consistent with the linear regression line of Figure 3. The Apollo 17 observations demonstrate the usefulness of HST in enabling high spatial and spectral resolution UV mapping of the lunar surface for scientific and resource-related applications. Future observations by the HST and the UV sensitive Lunar Reconnaissance Orbiter Wide Angle Camera (315 and 360 nm bandpasses) will provide the means to test the utility of UV mapping to determine compositional variations across the whole Moon.

[15] **Acknowledgments.** We gratefully acknowledge the contributions of the following individuals in making the complex HST lunar observations both possible and successful: Dave Leckrone (GSFC), Lisa Mazzuca (GSFC), Tony Roman (STScI), Don Lindler (GSFC), Max Mutchler (STScI), Charles Proffitt (STScI), Michael Moore (NASA HQ), Paul Hertz (NASA HQ), and many others at GSFC, Lockheed-Martin, and ST ScI HST Operations team. P. Lucey (Univ. HI) provided insightful comments that certainly improved this manuscript. Portions of this work were supported under the NASA Planetary Geology and Geophysics grant NNG05GG64G.

References

Bell, J. F., III, M. J. Wolff, P. B. James, R. T. Clancy, S. W. Lee, and L. J. Martin (1997), Mars surface mineralogy from Hubble Space Telescope imaging during 1994–1995: Observations, calibration, and initial results, *J. Geophys. Res.*, *102*, 9109–9123.

Charette, M. P., T. B. McCord, C. M. Pieters, and J. G. Adams (1974), Application of remote spectral reflectance measurements to lunar geology classification and determination of titanium contents of lunar soils, *J. Geophys. Res.*, *79*, 1605–1613.

Gillis-Davis, J. J., P. G. Lucey, and B. R. Hawke (2006), Testing the relation between UV-vis color and TiO_2 content of the Lunar Maria, *Geochim. Cosmochim. Acta*, *70*, 6079–6102, doi:10.1016/j.gca.2006.08.035.

Hapke, B. (2001), Space weathering from Mercury to the asteroid belt, *J. Geophys. Res.*, *106*, 10,039–10,073.

Hapke, B., W. Cassidy, and E. Wells (1975), Effects of vapor-phase deposition processes on the optical, chemical, and magnetic properties of the lunar regolith, *Moon*, *13*, 339–353.

Lucchitta, B. K. (1972), Geologic map of part of the Taurus-Littrow region of the Moon, Apollo 17 pre-mission map, scale 1:50,000, sheet 2, *U.S. Geol. Surv.*, *Map I-800*.

Lucey, P. G., D. T. Blewett, G. J. Taylor, and B. Ray Hawke (2000), Images of lunar surface maturity, *J. Geophys. Res.*, *105*, 20,297–20,305.

Pavlovsky, C., et al. (2002), ACS instrument handbook, version 3.0, public document, Space Telesc. Sci. Inst., Baltimore, Md.

Pieters, C. M. (1978), Mare basalt types on the front side of the Moon: A summary of spectral reflectance data, *Proc. Lunar Planet. Sci. Conf.*, *9th*, 2825–2849.

Pieters, C. M., L. A. Taylor, S. K. Noble, L. P. Keller, B. Hapke, R. V. Morris, C. C. Allen, D. S. McKay, and S. Wentworth (2000), Space weathering on airless bodies: Resolving a mystery with lunar samples, *Meteorit. Planet. Sci.*, *35*, 1101–1107.

Robinson, M. S., and B. L. Jolliff (2002), Apollo 17 landing site: Topography, photometric corrections, and heterogeneity of the surrounding highland massifs, *J. Geophys. Res.*, *107*(E11), 5110, doi:10.1029/2001JE001614.

Robinson, M. S., E. Malaret, and T. White (2003), A radiometric calibration for the Clementine HIRES camera, *J. Geophys. Res.*, *108*(E4), 5028, doi:10.1029/2000JE001241.

Wagner, J. K., B. W. Hapke, and E. N. Wells (1987), Atlas of reflectance spectra of terrestrial, lunar, and meteoritic powders and frosts from 92 to 1800 nm, *Icarus*, *69*, 14–28.

Wells, E., and B. Hapke (1977), Lunar soil: Iron and titanium bands in the glass fraction, *Science*, *195*, 977–979.

Whitaker, E. A. (1972), Lunar color boundaries and their relationship to topographic features: A preliminary survey, *Moon*, *4*, 348–355.

J. F. Bell III, Department of Astronomy, Cornell University, 610 Space Science Building, Ithaca, NY 14853-6801, USA.

J. B. Garvin and D. Skillman, NASA Goddard Space Flight Center, Code 924, Greenbelt, MD 20771, USA.

B. W. Hapke, Department of Geology and Planetary Science, University of Pittsburgh, 200 SRCC Building, 4107 O'Hara Street, Pittsburgh, PA 15260, USA.

C. M. Pieters, Department of Geological Sciences, Brown University, P.O. Box 1846, Providence, RI 02912, USA.

M. S. Robinson, School of Earth and Space Exploration, Arizona State University, Box 871404, Tempe, AZ 85287-1404, USA. (mrobinson@asu.edu)

M. P. Ulmer, Department of Physics and Astronomy, Northwestern University, 2145 Sheridan Road, Evanston, IL 60208-3112, USA.